IOP Conf. Series: Journal of Physics: Conf. Series **871** (2017) 012049 doi:10.1088/1742-6596/871/1/012049

Magnetic flux invasion in REBCO bulk magnets with varying pre-magnetized flux distributions in multiple-PFM processes

T Oka[1], K Hara[1], A Takeda[1], J Ogawa[1], S Fukui[1], T Sato[1], K Yokoyama[2] and A Murakami[3]

[1] Niigata University, 8050 Ikarashi-Ninocho, Nishi-Ward, Niigata 950-2181, Japan
[2] Ashikaga Institute of Technology, 268-1 Ohmae-cho, Ashikaga, Tochigi 326-8558, Japan
[3] Ichinoseki National College of Technology, Takanashi, Hagisho, Ichinoseki, Iwate 021-8511, Japan

okat@eng.niigata-u.ac.jp

Abstract. The motion of magnetic flux invading into the HTS bulk magnets were experimentally studied in their pulsed field magnetization processes. The authors paid attention to the effects of the shapes of the pre-magnetized trapped flux distributions before the successive field applications by means of varying the M-shaped distribution. We estimated the differences of the magnetic flux motions between the Dy123 and Gd123 systems, which might have different J_c properties of each sample. As for the Dy123 system, the increase of remaining flux in the periphery region of the M-shaped distribution resulted in the decrease of flux-trapping according to the promotion of flux invasion. On the other hand, trapped flux density has been raised to 3.4 T owing to the effective suppression of flux invasion for the Gd123 bulk magnet. The experiments showed that the peak heights and the positions of the formerly trapped M-shaped fluxes precisely affect the heat generation and the trapped field performance.

1. Introduction

It is well-known that the largely-grown RE–Ba–Cu–O (RE = Y, Sm, Dy, Gd, as RE123) high temperature superconductors (abbreviated as HTS), which are fabricated by the so-called melt-process behave as the trapped field magnets or the bulk magnets [1], [2]. Recently, the world high trapped field of 17.6 T has been reported by Durrell *et al.* [3] by means of the field cooling (FC) process accompanied with a large scale superconducting solenoid magnet and under the special reinforcement to promote mechanical strength of the bulk magnet against the fracture stress due to the magnetic force caused by the strong pinning effect. Although the performances of the trapped fields in FC clearly express the potential abilities of their magnetic field emission, the usage of large scale superconducting magnets would have to limit the application areas for the bulk magnets. While the field trapping ability is usually evaluated in the FC process, various kinds of pulsed field magnetization methods (abbreviated as PFM) have been developed as more compact and practical magnetization methods than FC.

On the course of PFM process, the flux motion in the sample causes the local heat, raises the temperature, lowers the critical current density, and resultantly degrades the trapped field ability [4]. Mizutani *et al.* [5] showed that the iterative application of pulsed fields applied at low temperature regions beneath 77 K is effective for enhancing the trapped field in the bulk magnets. In the past, some other studies have clarified that the existing magnetic flux beforehand in the bulk magnet substantially affects the magnetic flux invasion in the following pulsed field application. Sander *et al.* [6] reported

that iterative pulse field application with lowering the sample temperature is effective to promote the trapped field. In 2005, Fujishiro *et al*. [7] reported the strongest field trapping of 5.2 T for the first time in the world by MMPSC method they call, applying iterative pulsed fields at two different temperature stages at 47 K and 28 K.

In the study, the authors take a couple of approaches to promote the field trapping ability of the bulk magnets. One is the approach on the material fabrication. The authors have reported the fabrication of the twin-seeded samples and the anisotropic flux motion in the field application processes [8]. Since the applied magnetic fluxes invade into the bulk magnets from outside to the sample centre, we must take the shape of samples [9] or pulse coils [10], macroscopic grain structure [11], angle dependence [12], the macroscopic defects in the samples [13, 14] into account when we design the activation systems.

The other approach is on the field application method, considering such as the intensity, iterative number, temperature to control the flux motion, heat generation [15]. In the paper, we focus on the shapes of the existent magnetic flux which was trapped beforehand the successive field applications. With use of densely-fabricated Dy123 and Gd123 bulk magnets, we estimated the flux motion and field trapping ability during and after various iterative PFM modes. We aim to clarify the magnetic flux behavior in the PFM operations to improve the field trapping property.

2. Experimental procedure

2.1. Bulk magnets

Figure 1(a) shows a photograph of the melt-processed Dy123 bulk sample manufactured by Nippon Steel and Sumitomo Metals Co. LTD with the dimensions of 30 mm in diameter and 15 mm in thickness. As employed was the unique heat treatment which was operated in the oxygen atmosphere, the mechanical strength of thus densely-made sample was substantially promoted by reducing internal voids [16]. A top view of the sample shows us that the crystal growth begins from the seed crystal attached at the centre toward the periphery of the sample. One sees the obvious traces of crystal growth and the cross-shaped lines showing like the boundaries, which we call growth sector boundaries GSB and growth sector regions GSR. The Gd123 bulk magnet with the same shape in dimensions was employed as a comparison with Dy123 system. The systems have different properties with each other mainly with respect to their J_c values. In Figure 1(b), the positions of the Hall sensor are indicated at four positions (r = 0, 3, 6, 9 mm) to detect the flux motion during and after the PFM processes. They were changed in order in the same manner on each PFM process.

2.2. Experimental setup

Figure 1(c) schematically shows the whole equipment which was employed in this study. The experimental procedure is shown elsewhere [15, 17]. The bulk magnet is cooled to the lowest temperature of 30 K by a Gifford-McMahon refrigerator (AISIN SEIKI Co., GR-103). The successive magnetic fields around 5-7 T were generated and applied to the Dy123/Gd123 bulk magnets by feeding currents to the pulse coil from the condenser bank (SBV-10124, Nihon Denji Sokki Co). The changes

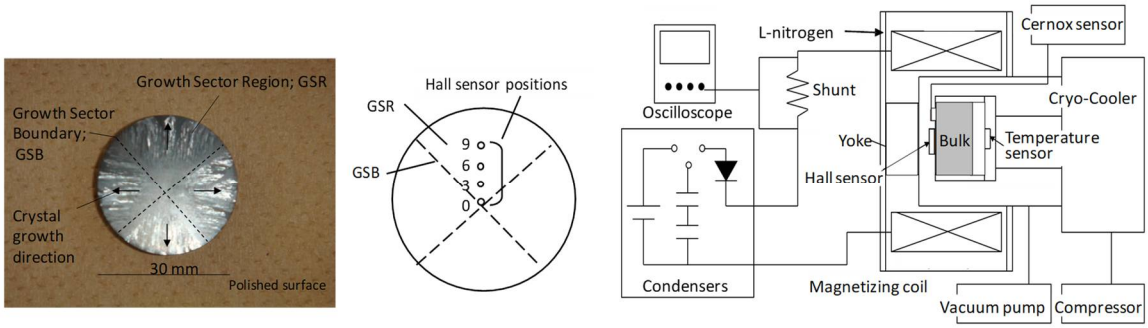

(a) (b) (c)

Figure 1. A surface view of Dy123-based bulk magnet (a), the Hall sensor positions on it (b), and the schematic illustration of the whole experimental setup for pulsed field magnetization (c).

of the magnetic flux density were measured at various points on the bulk magnet surface during and after every magnetizing procedure, as shown in Figure 1(b). The magnetizing electrical circuit is composed of a condenser bank, a shunt resistor, and a 112-turn pulse coil. The cross section of copper wire is 3.0×1.24 mm^2, which is dipped in the liquid nitrogen vessel to reduce the resistance by cooling it to 77 K. The coil constant is 0.925 mT/A. An iron yoke is attached to the bulk magnet to attract the magnetic flux during the pulsed field application.

3. Results and Discussion

3.1. Successive-PFM processes in various pre-shaped magnetic flux distributions

It is reported that the remnant trapped field distributions affects the successive magnetic flux application and their field-trapping behaviours [18, 19]. The authors paid attention to the pre-shaped magnetic flux distributions in the successive PFM operations. Various pre-shaped distributions were formed at the centre of the bulk magnet. Figure 2 shows the trapped flux distributions before (a) and after (b) 7-T application in the successive-PFM processes of 5(40K)-5-7, 5-5-7, and 6-5-7T. The data were measured at r=0-9 mm on the bulk surface, and were plotted on the x-axis which was reflected at the y-axis in each plot area. The legends show the order of the pulsed field applications.

As shown in Figure 2, we obtained various pre-shaped flux distributions by various successive field applications at the center of the sample, while the same distribution was observed at the periphery of the sample. Although the final flux trapping was insufficient when we took the concave distribution at the centre portion, the steep and fine conical flux distributions were obtained when we formed the pre-activated trapezoid shapes. The pre-shaped flux distribution is found to affect the final trapped field distribution. As shown in Figure 3, we exhibit the same flux distributions as shown in Figure 2, and compare it with those of the sample which has weak flux distribution on the periphery. The trapped field apparently degraded at the centre portion in comparison with Figure 2. On the other hand, although the same flux distributions were formed at the periphery, insufficient flux trapping there resulted in the insufficient flux invasion into the centre portion of the bulk magnet.

Figure 4 shows the data of increasing speed (T/s) of the magnetic flux penetration, which corresponds to Figures 2 and 3. The data were derived from the inclination in each time-evolutional profile measured at the centre surface during the 7-T PFM operation. Among the group of 50-70 T/s, the data of 5-5-7 T field application only shows the extremely rapid motion of around 140 T/s. This suggests that the changes of the magnetic flux at the centre portion related to the heat generation and degradation of J_c values. The pre-shaped flux distribution apparently affects to the successive field application and resultant flux trapping ability.

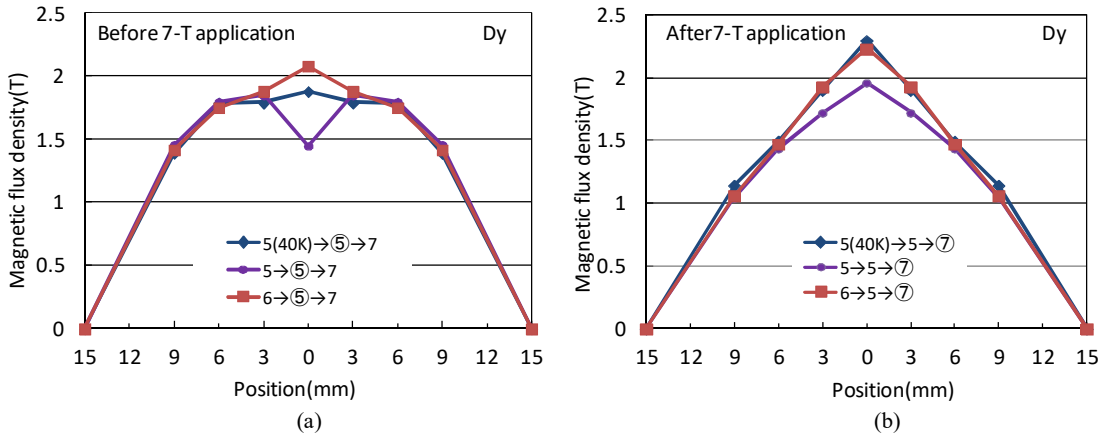

Figure 2. Trapped field distributions before 7-T application (a) and after (b) for the various field distribution shapes formed at the centre before the applications.

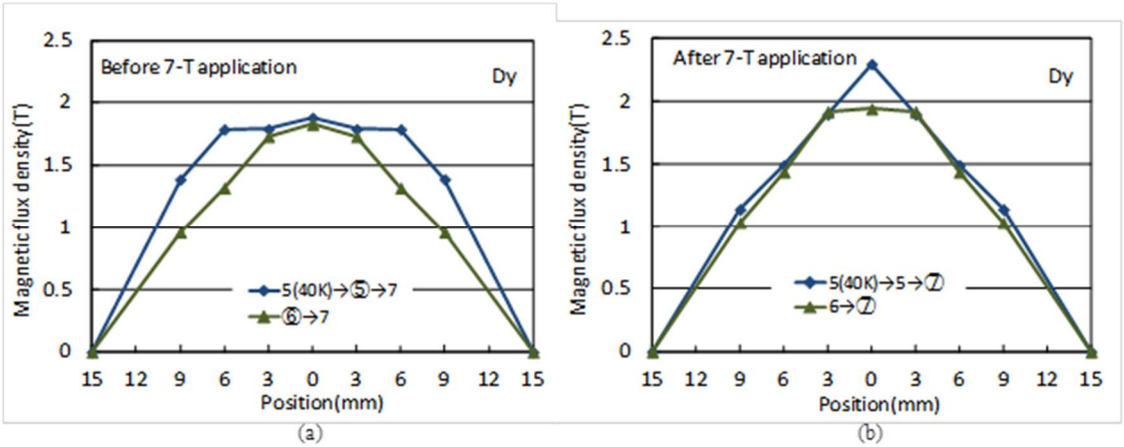

Figure 3. Trapped field distributions before 7-T application (a) and after (b) for the various field distribution shapes formed at the periphery of the sample before the applications.

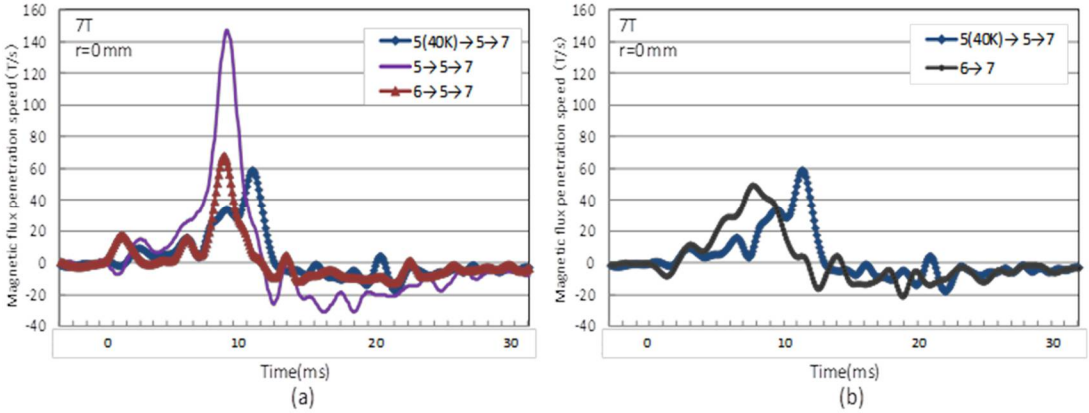

Figure 4. Time evolution profiles of magnetic flux penetration speeds for the distribution-shape varieties shown at the and during 7-T application for the various field distribution shapes formed at the centre (a) and at the periphery (b) before the applications.

3.2. Successive-PFM in various M-shaped flux trapping

According to the Fujishiro's report [20], the pre-activated "M-shaped" flux distribution was proved to be effective for high-field trapping. We investigated the flux trapping performance and the magnetic flux motion which were affected by various M-shaped flux distribution on the sample periphery. The Gd123-based sample was employed in addition to Dy123 bulk magnet. Figure 5 shows four types of the pre-activated M-shaped flux distributions. Various pre-shaped flux distributions were prepared on their periphery with the same magnetic flux trapping of 1.5 T at the centre portion on the sample surface.

The changes of the flux invasion into the sample during the final 7-T application are plotted in Figure 6. In Dy system, the flux shows the sluggish invasion on its periphery, and the applied flux lately invades in comparison to other areas. This means that the existent magnetic flux apparently restricts the flux invasion.

On the other hand, the flux invasion was stopped at the periphery in Gd system, as shown in Fig. 5b, whereas the field invasion in the case of 5-7 application was enhanced, as shown in Fig. 6b. Therefore, the existent M-shaped distribution promotes the flux invasion in the case of 5-7 application, and lowers the trapped field in comparison with single 7-T application. We observe the promotion of flux invasion and restriction of heat generation when we apply the 5-5-7 T with the substantial flux trapping on its periphery.

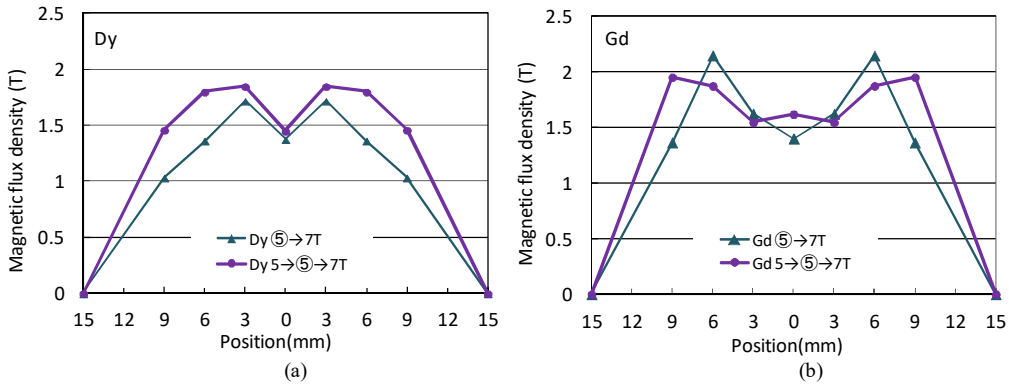

Figure 5. Trapped field distributions before 7-T application for Dy123 (a) and Gd123 (b).

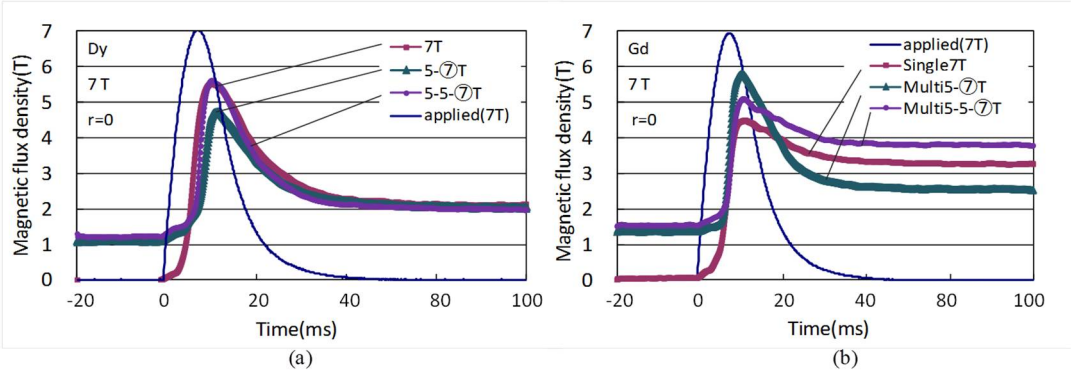

Figure 6. Time evolutional profiles of magnetic flux invasions into Dy123 (a) and Gd123 (b) during 7-T application.

Figure 7 shows the resultant trapped flux distributions after final 7-T application to various pre-activated M-shaped Gd123 system. The highest trapped flux of 3.43 T was obtained when the 5-5-7 successive fields were applied, which showed the fine conical distribution. Although we see no differences at each peripheral flux trapping, we observe various trapped flux distributions which correspond to the respective pre-activated M-shape at the centre portion.

Figure 8 shows the magnetic flux penetration speeds measured at the centre. In the Dy system, the flux invasion for 5-7 and 5-5-7 data occurs late in comparison with single 7-T application, which relates the weak and sluggish penetration into the sample. In case of Gd, the slight excess speed for 5-7 application might result in the higher heat generation and lower flux trapping at the centre part. The discussion of heat generation would have to wait the results of the direct temperature measurement on each position of the sample surface. The trapped flux performances are listed in Table 1. The final

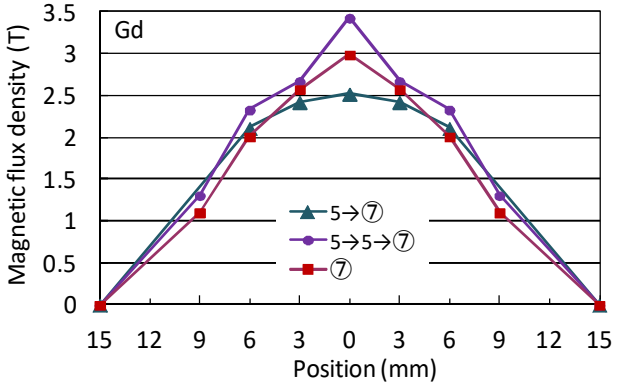

Figure 7. Trapped field distributions after 7-T application for Gd123.

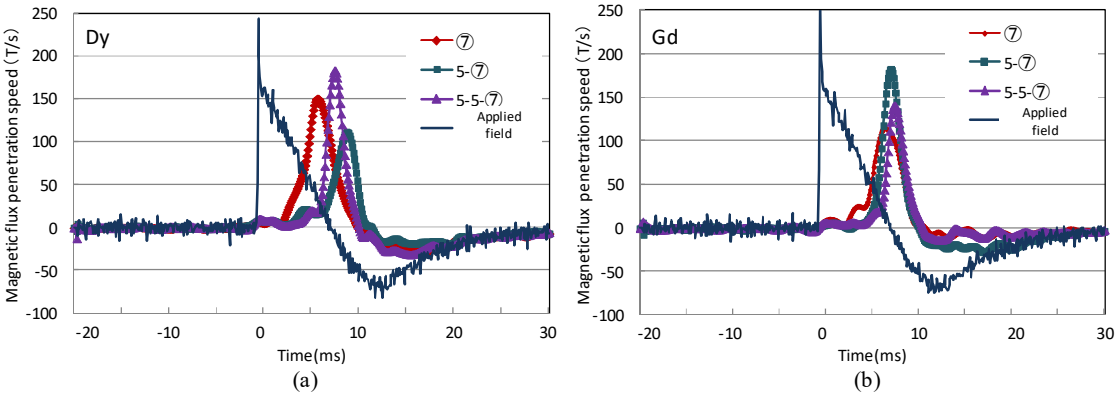

Figure 8. Magnetic flux penetration speeds for Dy123 (a) and Gd123 (b) during 7-T application to the sample showing different M-shaped distributions.

Table 1. Final trapped fields after various activation modes.

System	7	5-7	5-5-7
Dy	1.87	2.07	2.06
Gd	2.99	2.52	3.43

The data were measured at the center of the bulk surface [T].

trapped flux is finely found to correspond to the pre-shaped flux distribution. One can see distinctive difference in the flux trapping ability between Dy and Gd systems, which clearly reflects the J_c performances of the samples chosen.

4. Conclusion

We precisely investigated the effects of applied magnetic flux invasion to the pre-activated samples of Dy and Gd123 systems having various M-shaped flux distributions. The bulk magnets trap the substantial remnant flux on the periphery areas of the samples, and the distributions relax the field gradient when the successive pulsed-field was applied. This phenomenon is capable of suppress the flux motion and heat generation. The final flux invasion tends to be promoted when the steep M-shaped distribution is formed. When we form the weak magnetic field area showing M-shape at the centre portion, the successive applied flux invades toward the centre portion without any blocking by the pre-activated magnetic flux.

Acknowledgments

The bulk sample was supplied by Dr. Teshima in Nippon Steel and Sumitomo Metal Co. The authors give him great thanks for the courtesy.

References

[1] Wipf S and Laquer H 1989 *IEEE Trans. Magn.* **25** 1877
[2] Tomita M and Murakami M 2003 *Nature* **421** 517
[3] Durrell J, Dennis A, Jaroszynski J, Ainslie M, Palmer K, Shi Y-H, Campbell A, Hull J, Strasik M, Hellstrom E and Cardwell D 2014 *Supercond. Sci. Technol.* **27** 082001
[4] Itoh Y and Mizutani U 1996 *Jpn. J. Appl. Phys.* **35** 2114
[5] Mizutani U, Ikuta H, Hosokawa T, Ishihara H, Tazoe K, Oka T, Itoh Y, Yanagi Y and Yoshikawa M 2000 *Supercond. Sci. Technol.* **13** 836
[6] Sander M, Sutter U, Koch R and M. Klaeser M 2000 *Supercond. Sci. Technol.* **13** 841
[7] Fujishiro H, Tateiwa T, Fujiwara A, Oka T and Hayashi H 2006 *Phys. C*. **445-448** 334

[8] Oka T, Miyazaki T, Ogawa J, Fukui S, Sato T, Yokoyama K and Langer M 2015 *Supercond. Sci. Technol.* **29** 024003
[9] Tateiwa T, Sazuka Y, Fujishiro H, Hayashi H, Nagafuchi T and Oka T 2007 *Phys. C.* **463-465** 398
[10] Ida T, Matsuzaki H, Akita Y, Izumi M, Sugimoto H, Hondou H, Kimura Y, Sakai N, Nariki S, Hirabayashi I, Miki M, Murakami M and Kitano M 2004 *Phys. C* **412-414** 638
[11] Fujishiro H, Arayashiki T, Tamura T, Naito T, Teshima H and Morita M 2012 *Jpn. J. Appl. Phys.* **51** 093005
[12] Ainslie M, Zou J, Mochizuki H, Fujishiro H, Shi Y-H, Dennis A and Cardwell D 2015 *Supercond. Sci. Technol.* **28** 125002
[13] Yokoyama K, Oka K, Kondo N and Hosaka S 2013 *Phys. C* **484** 343
[14] Fujishiro H, Naito T and Oyama M 2012 *Phys. Procedia* **36** 687
[15] Oka T, Ota H, Shimoda T, Ogawa J, Fukui S, Sato T, Yokoyama K, Murakami A and Langer M 2014 *IEEE Trans. on Appl. Supercond.* **25** 6800904
[16] Murakami A, Miyata H, Hashimoto R, Otaka K, Katagiri K and Iwamoto A 2009 *Phys. C* **469** 1207
[17] Yanagi Y, Itoh Y, Yoshikawa M, Oka T, Ikuta H and Mizutani U 2005 *Supercond. Sci. Tech.* **18** 839
[18] Oka T, Seki H, Ogawa J, Fukui S, Sato T and Yokoyama K 2011 *IEEE Trans. Appl. Supercond.* **21** 3356
[19] Oka T, Ishiduka D, Otsuka T, Ogawa J, Fukui S, Sato T, Yokoyama K and Murakami A 2013 *J. Supercond. Nov. Magn.* 26 1301
[20] Fujishiro H, Hiyama T, Tateiwa T, Yanagi Y and Oka T 2007 *Phys. C* **463–465** 394